Postpressing dependence of the effective electron diffusion coefficient in electrophoretically prepared nanoporous ZnO and TiO_2 films

S. Dor
Department of Chemistry, Nano-Energy Research Center, Institute of Nanotechnology and Advanced Materials, Bar-Ilan University, Ramat-Gan 52900, Israel

Th. Dittrich
Hahn-Meitner-Institute, 14109 Berlin, Germany

A. Ofir, L. Grinis, and A. Zaban[a)]
Department of Chemistry, Nano-Energy Research Center, Institute of Nanotechnology and Advanced Materials, Bar-Ilan University, Ramat-Gan 52900, Israel

(Received 12 November 2007; accepted 28 December 2007)

The porosity of electrophoretically prepared nanoporous ZnO and TiO_2 films was systematically decreased by postpressing at different pressures. The nanoporous structure of the films was fixed by sintering after the postpressing procedure. The postpressing-induced change of the internal surface area of the nanoporous films was monitored using the dye-removal technique. The effective electron diffusion coefficient (D_{eff}) of the unpressed nanoporous films depended on the thickness according to Fick's second law. When pressed, the diffusion coefficient of the films increases significantly. In nanoporous TiO_2, the increase of D_{eff} follows the percolation theory where transport rate depends on the particle-coordination number. In contrast to the TiO_2 films, the value of D_{eff} of pressed nanoporous ZnO films changed with the porosity much stronger than one would expect from the percolation theory with hard spheres. This property has been attributed to the strong increase of necking between ZnO nanoparticles with increasing pressure as indicated by a strong decrease of the internal surface area.

I. INTRODUCTION

Two of the main transparent n-type semiconductors materials that are used as electron-conducting medium in dye-sensitized solar cells (DSSCs) are TiO_2 and ZnO. Use of their nanostructure provides a large internal surface area, which is necessary for dye molecules adsorption, thereby leading to sufficient high light absorption.[1–3] The potentials of the valance band maximum and the conduction band minimum of those materials are close, which explains their ability to function under the energy level restriction of the other components in dye-sensitized solar cell system. The main advantage of ZnO over TiO_2 is the ability to form preferred morphologies that can enhance the transport properties of the electron.[4] However, at least to date, the reported performance of DSSCs composed from TiO_2 nanoporous film is superior over those made by ZnO.[5,6]

Electron transport throughout a nanoporous film is strongly influenced by the film morphology.[7,8] Nanoporous layers of metal oxide nanoparticles can be prepared by electrophoretic deposition (EPD).[9] The implementation of the EPD process allows a systematic modification of the morphology of the films by applying mechanical press before fixing the structure by sintering. Changes of the morphology are given mainly by the decrease of the porosity after pressing. The decrease of the porosity leads to an increase of the mean coordination number of nanoparticles and therefore to an increase of percolation in the nanoporous film resulting in an increase of the effective electron diffusion coefficient (D_{eff}). In previous work, we showed the influence of porosity on D_{eff} in TiO_2 nanoporous films.[9,10] Pressing of nanoparticle films leads also to an increase of the contact area between nanoparticles and therefore to a decrease of the internal surface area of the nanoporous film. The hardness of the nanoparticles together with the pressure determines the increase of the contact area. Obviously, the electron transport depends on the increase of the contact area as well.

a)Address all correspondence to this author:
e-mail: zabana@mail.biu.ac.il
DOI: 10.1557/JMR.2008.0116

 © 2008 Materials Research Society

In this work we compare the effective electron diffusion coefficients of nanoporous ZnO and TiO_2 electrodes modified by postpressing at different pressures. TiO_2 nanoparticles can exist in a rutile or anatase phases. TiO_2 is much harder than ZnO. For example, the hardness values of ZnO and rutile on the Mohs hardness scale are 4.0 and 6.3, respectively.[11] Therefore, it will be possible to get more information about the role of the contact area between nanoparticles for the diffusion process. The nanoporous electrodes are characterized by measuring the surface area using dye-removal techniques and by transient photocurrent measurements in electrolyte.

II. ANALYSIS OF THE EFFECTIVE DIFFUSION COEFFICIENT

Nanoporous electrodes were prepared by EPD at different deposition times to check the general behavior of D_{eff} of unpressed electrodes. Photocurrent transients are excited from the external surface of the nanoporous film and exhibit a typical diffusion peak. The value of D_{eff} is determined by the effective thickness (L_{eff}) of the nanoporous film and by the time at which the maximum photocurrent is reached (t_{peak}).

$$D_{\text{eff}} = \frac{{L_{\text{eff}}}^2}{6 \cdot t_{\text{peak}}} \quad . \tag{1}$$

The value of L_{eff} is less than the film thickness (L) because of penetration of exciting light into the near surface region of the nanoporous film (equal to the inverse absorption coefficient α^{-1}). Usually the value of α^{-1} is well known for the material of the nanoparticles. The value of L_{eff} can be estimated by taking into account the porosity (P) of the nanoporous film:

$$L_{\text{eff}} = L - \frac{\alpha^{-1}}{1 - P} \quad . \tag{2}$$

The porosity of the unpressed films (P_{un}) was determined by weighing and from the volume of the films. It has been found that P_{un} is independent of the deposition time. The porosity of pressed films (P_{p}) was found by comparing the thickness of the pressed film (L_{p}) with the thickness of the unpressed film (L_{un}):

$$P_{\text{p}} = \frac{L_{\text{p}} - (1 - P_{\text{un}}) \cdot L_{\text{un}}}{L_{\text{p}}} \quad . \tag{3}$$

According to percolation theory the porosity dependence of the D_{eff} can be described by

$$D_{\text{eff}} = D_0 \cdot |P - P_{\text{C}}|^{\beta} \quad , \tag{4}$$

where D_0 is a constant containing information on the average distance between the particles, P is the film porosity, P_{c} is the critical porosity (percolation threshold, $P_{\text{C}} = 0.76$ for the nanoporous materials or cubic three-dimensional (3D) lattice[12–14]), and β is a power coefficient.[15]

III. EXPERIMENTAL

A. Electrode preparation

Nanoporous ZnO (Sigma-Aldrich, Germany, nanopowder ~60 nm) and TiO_2 (P25, Degussa ~25 nm) (Evonik Degussa Corp., Parsippany, NJ) films were fabricated by the EPD technique developed in our lab and described elsewhere by Grinis et al.[9] EPD enables simple preparation of uniform, free-binder films with controlled thickness and with high reproducibility. Another advantage of the technique is that the porosity is independent of the layer thickness. The initial porosities of the unpressed films were 0.6 for the TiO_2 and 0.52 for the ZnO.

The ZnO and TiO_2 particles were deposited on a conducting SnO_2:F glass (TEC-15) (Pilkington Group Ltd., St. Helens, WA). The film thicknesses were measured with a profilometer (SV 500, Mitutoyo Co., Japan). For the photocurrent transient measurement two different series were prepared: (i) series of unpressed nanoporous electrodes with thickness variation by EPD deposition time, (ii) series of pressed nanoporous electrodes with fixed initial thicknesses and pressure variations. For example, for nanoporous ZnO a series of six unpressed electrodes was prepared with film thicknesses in the range between 0.2 and 1 μm and a series of five pressed electrodes were fabricated with identical initial film thickness and pressures of 0.0, 0.2, 0.4, 0.6, and 0.8 ton/cm^2. As the final preparation step the nanoporous electrodes were sintered in air at 500 °C for 30 min.

B. Pressure treatment

A hydraulic programmable press (Bivas Hydraulic Industries Ltd., Petah Tikva, Israel) was used for pressing the films after the EPD. The pressing process was at room temperature, and the maximum applied pressure was 0.8 t/cm^2. The detailed pressing procedure is described elsewhere.[9] Figure 1 shows some examples for the change of the thickness caused by pressing of nanoporous ZnO or TiO_2 electrodes. The change of the thicknesses with increasing pressure is very similar for nanoporous ZnO and TiO_2 electrodes. The relative change of the thickness is larger for thicker electrodes. The porosities can be calculated using Eq. (3). For example, the porosity of unpressed nanoporous ZnO electrodes (initial film thickness 4.3 μm) amounts to 0.52, and the porosities of the electrodes pressed at 0.2, 0.4, 0.6, and 0.8 t/cm^2 are 0.46, 0.39, 0.31, and 0.23, respectively.

C. Photocurrent transients measurement

Photocurrent transients were excited with pulses of a N_2 laser (337 nm, 5 ns, repetition rate 1 Hz). A transient measurement system with logarithmic readout

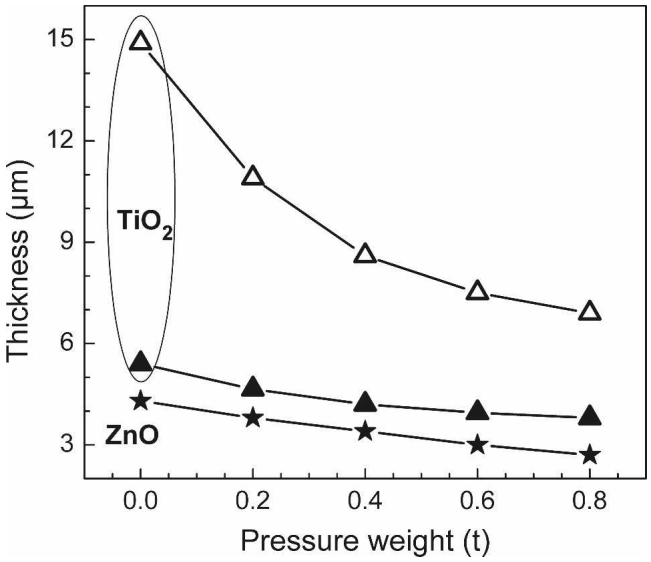

FIG. 1. Examples for the change of the thickness due to pressing of nanoporous ZnO or TiO_2 (two different initial thicknesses) electrodes.

(800 points/pulse) and with a logarithmic increment of averaging over neighbored data points has been used (100 Ms/s, 14 bit resolution, 10^8 samples, Gage) (Gage Applied Technologies, Lockport, IL). For the photocurrent measurements, the electrodes were immersed in a 0.5 M NaCl electrolyte (pH = 2, HCl). Illumination was performed from the electrolyte side and the SnO_2:F back contact was grounded. The measurement resistance was 50 Ω. The nanoporous ZnO layers are not stable for a long time in the used electrolyte due to etching of ZnO in acidic solution. The logarithmic measurement system allowed us to obtain one transient with one laser pulse so that one measurement was performed within 30 s after immersing the sample into the electrolyte. During this time, the samples could be considered stable. Figure 2 shows photocurrent transients of a nanoporous ZnO electrode measured immediately after immersion into the electrolyte and measured after 4 and 8 min of etching in the electrolyte. Etching leads to an increase of surface defects and therefore to a decrease of the integrated charge, i.e., to an increase of recombination. Further the value of t_{peak} shifts to longer times with increasing immersion time because of increasing porosity.

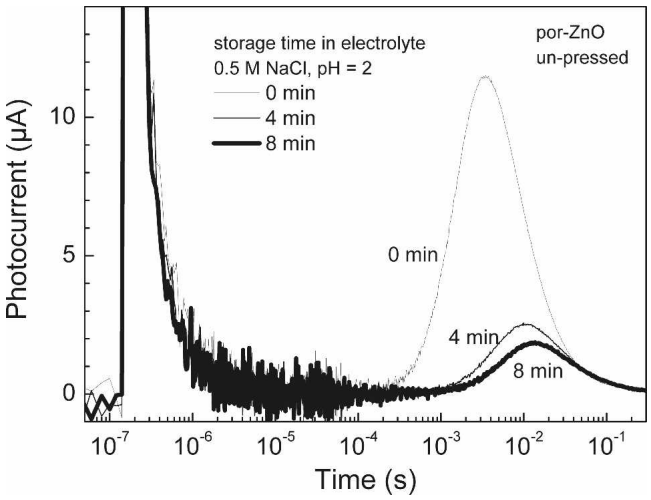

FIG. 2. Photocurrent transients of a nanoporous ZnO electrode measured in acidic solution after different times.

D. Surface area measurement

Surface area measurement was done using a dye-removal technique. Electrodes with known geometrical area were overnight soaked in ethanol solution of 10 mM N3 dye (Solaronix, Switzerland). The N3 dye was then removed from each electrode using identical amounts of NaOH 1 M aqueous solution. The concentrations of the solutions with the removed dye were measured by optical absorption at the wavelength of 530 nm. The obtained values of absorbance were divided by the geometrical area of the electrode and normalized to the value of the unpressed electrodes. Figure 3 compares the normalized internal surface areas of some pressing series of nanoporous TiO_2 and ZnO electrodes as a function of the normalized thickness. The internal surface area decreases monotonously to up to 80% of the unpressed TiO_2 and to up to 50% of the unpressed ZnO electrodes for maximal pressures. This strong difference is caused by the different hardness of TiO_2 and ZnO.

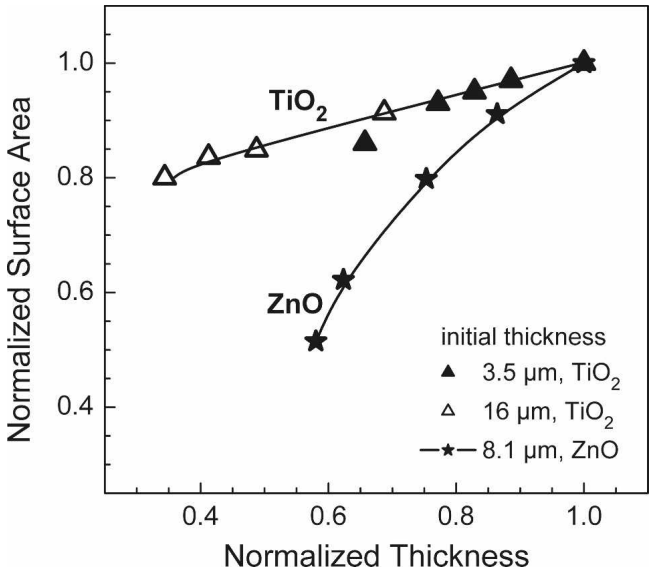

FIG. 3. Dependence of the normalized internal surface area on the normalized thickness for pressing series of nanoporous TiO_2 and ZnO electrodes on the normalized thickness. The points correspond to pressures of 0.0, 0.2, 0.4, 0.6, and 0.8 t/cm^2.

IV. RESULTS AND DISCUSSION

Figure 4 shows typical photocurrent transients for unpressed nanoporous ZnO electrodes deposited at different times during EPD. The layer thickness increases proportional to time. The value of t_{peak} increases with increasing layer thickness as expected. The integrated charges of the photocurrent transients given in Fig. 4 are independent of the deposition time amounting to 0.21 ± 0.05 μC.

The dependence of t_{peak} on the film thickness is given in Fig. 5 for unpressed nanoporous ZnO and TiO_2 electrodes. The slopes in the log–log plots are two that correspond to D_{eff} independent of the film thickness. Therefore, it can be concluded that the fixed morphology of the deposited by EPD nanoporous films is similar in all films. For the series given in Fig. 5, the values of D_{eff} are 1.5×10^{-6} and 8×10^{-7} cm^2/s for unpressed nanoporous TiO_2 and ZnO electrodes, respectively. These values agree well with earlier measurements on nanoporous electrodes (for example, Ref. 6).

Pressing changes both film thickness and morphology. Figure 6 depicts photocurrent transients of pressed nanoporous ZnO electrodes. The values of t_{peak} shift toward shorter times with increasing pressure. The strongest change of the photocurrent transients has been observed between pressures of 0.4 and 0.6 t/cm^2. In this interval the value of t_{peak} decreases by one order of magnitude, and the integrated charge of the photocurrent transients increases by about 50%, which is significantly larger than the error induced by the measurements. At pressures higher than 0.6 t/cm^2, the value of t_{peak} decreases only marginally and the integrated charge of the photocurrent transients remain constant. The value of t_{peak} decreased by about two orders of magnitude from 27 ms for the unpressed film to 0.32 ms for the film that was pressed with the maximum applied pressure of 0.8 t/cm^2. Regarding the pressure-induced reduction of the film thickness (see Fig. 1) one would expect a decrease of t_{peak} of about three times after pressing at maximum pressure. This behavior is summarized in Fig. 7 for some dependencies of t_{peak} on the film thickness of pressed nanoporous TiO_2 and ZnO electrodes. It can be seen that the decrease of t_{peak} with decreasing film thickness of the pressed electrodes is much steeper than for unpressed electrodes (Fig. 5). Therefore, the value of D_{eff} of pressed nanoporous electrodes has to be obtained for each film thickness separately by using Eq. (1).

The values of D_{eff} and P have been obtained using Eqs. (1)–(3). For α^{-1}, a value of 200 nm (at the photon energy of 3.7 eV) has been used for the porous layers regarding absorption measurements on epitaxial anatase ($\alpha = 1.2 \times 10^5$ cm^{-1}) or rutile layers ($\alpha = 3 \times 10^5$ cm^{-1}).[16] As remark, the value of α^{-1} does not introduce a significant error since film thicknesses more than 4 μm

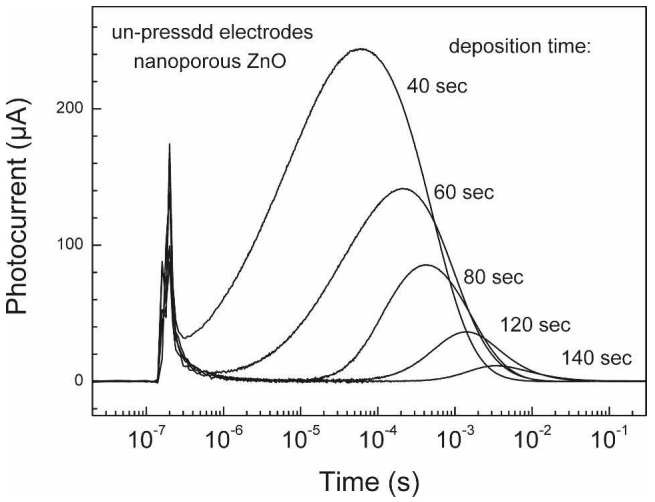

FIG. 4. Photocurrent transients obtained for unpressed nanoporous ZnO electrodes deposited by EPD at different times.

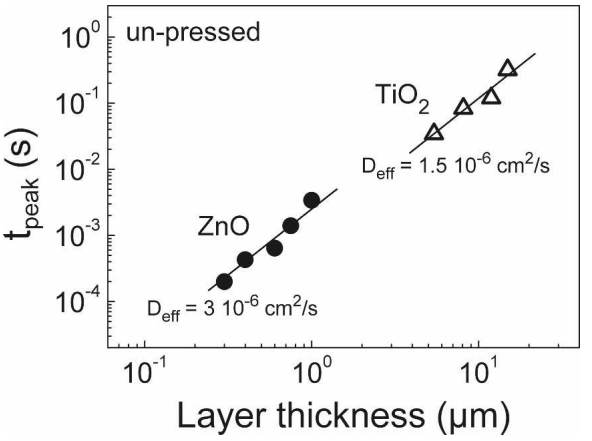

FIG. 5. Dependence of t_{peak} on the layer thickness of the unpressed nanoporous TiO_2 and ZnO electrodes.

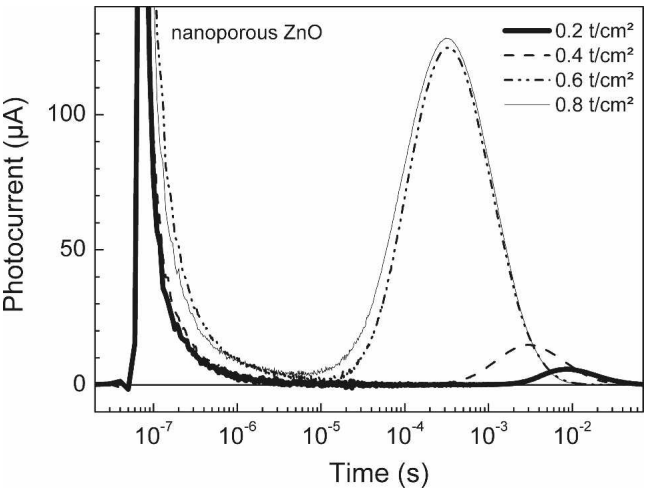

FIG. 6. Photocurrent transients of pressed nanoporous ZnO electrodes with initial layer thickness of 4.3 μm.

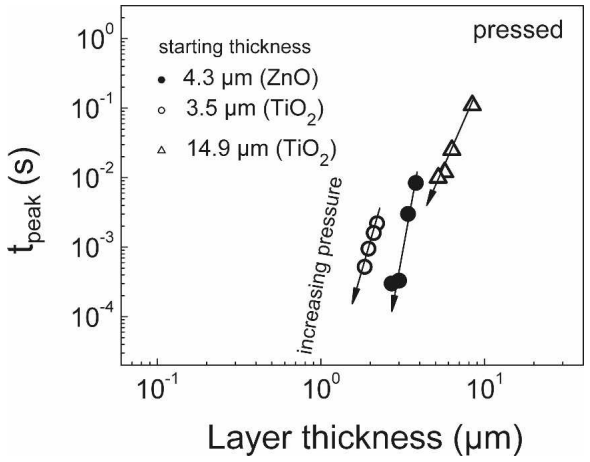

FIG. 7. Dependence of t_{peak} on the layer thickness of the pressed nanoporous TiO_2 and ZnO electrodes. The arrows give the direction of increasing pressure.

have been analyzed. Figure 8 summarizes the dependence of D_{eff} on $|P - P_C|$ for pressed nanoporous TiO_2 (a) and ZnO (b) films. For pressed nanoporous TiO_2 films, the value of D_{eff} changes by about five times from about 1.5×10^{-6} cm^2/s ($|P - P_C| = 0.25$) to about 7×10^{-6} cm^2/s ($|P - P_C| = 0.55$). The dependence of D_{eff} on $|P - P_C|$ follows a power law with a power coefficient of the order of 2 for pressed nanoporous TiO_2 films independent of the initial layer thickness. The percolation theories of Izyumov–Kirkpatrick[12,13] and Bernasconi–Wiesmann[14] show good agreement with Eq. (4) for low-porosity systems, provided $\beta \approx 2$, which is also the universal value for regular 3D lattices.

For pressed nanoporous ZnO films, the values of D_{eff} change by more than one order of magnitude from about 2×10^{-6} cm^2/s ($|P - P_C| = 0.31$) to about 3×10^{-5} cm^2/s ($|P - P_C| = 0.54$). It is interesting to note that the highest value of D_{eff} has been obtained after pressing at

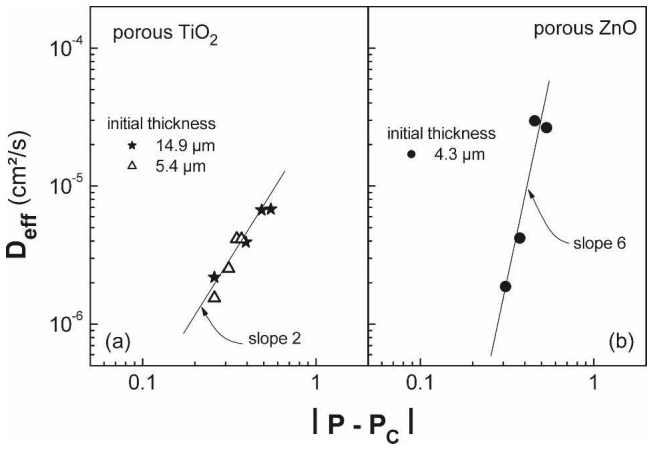

FIG. 8. Dependence of D_{eff} on the porosity of pressed nanoporous (a) TiO_2 and (b) ZnO electrodes. P_C is the critical porosity (0.76). The solid lines show the slopes of (a) 2 and (b) 6 as guides for the eye.

0.6 t/cm^2. Further, the dependence of D_{eff} on $|P - P_C|$ might be described by a function close to a power law regarding Eq. (4) but with $\beta \approx 6$. Such behavior cannot be explained by percolation theory based on hard spheres. Obviously, additional changes in morphology induced by pressing of nanoporous ZnO electrodes have to be considered.

The morphology dependence of D_{eff} in pressed nanoporous ZnO electrodes is rather complex. At one side, percolation improves with decreasing porosity, i.e., with increasing pressure. At the other side, the internal surface area decreases strongly with increasing pressure as shown previously (Fig. 3). This can be interpreted as an increase of the contact area between ZnO nanoparticles with increasing pressure that enables the charge transfer between neighbored nanoparticles. We assume that the strong increase of the contact area with increasing pressure is the reason for the strong deviations from predictions by percolation theory. However, D_{eff} decreased slightly after pressing at the maximum value compared with the lower value. This fact cannot be simply explained by uncertainties in the measurement procedure. ZnO nanoparticles started to modify under very high pressures. We believe that additional defects can be created at very high pressures, for example by the development of grain boundaries at interfaces between neighbored ZnO nanoparticles. Such mechanism would implement an upper limit for the improvement of D_{eff} by pressing.

V. CONCLUSION

It has been shown that the effective diffusion coefficient of nanoporous ZnO or TiO_2 electrodes prepared by electrophoretic deposition can be increased by postpressing after deposition but before fixing the structure by sintering. The pressing procedure leads to a decrease of the porosity and therefore to an improvement of percolation. The dependence of D_{eff} on $|P - P_C|$ follows quite well the predictions of percolation theory in the case of TiO_2 nanoparticles. For ZnO nanoparticles, additional factors such as increase of contact area between neighbored nanoparticles and deformation of nanoparticles have to be considered. For the given experimental conditions, an increase of D_{eff} by more than one order of magnitude has been reached for pressed nanoporous ZnO electrodes compared with unpressed electrodes. Our results indicate that pressing of nanoporous ZnO electrodes without annealing might be an option for low-temperature processing in photovoltaics.

ACKNOWLEDGMENT

The authors thank the Israeli Ministry of Infrastructure for the funding of this research.

REFERENCES

1. M.K. Nazeeruddin, A. Kay, I. Rodicio, R. Humphrybaker, E. Muller, P. Liska, N. Vlachopoulos, and M. Grätzel: Conversion of light to electricity by cis-X2-bis(2,2′-bipyridyl-4,4′-dicarboxylate)ruthenium(II) charge-transfer sensitizers (X = Cl^-, Br^-, I^-, CN^-, and SCN^-) on nanocrystalline TiO_2 electrodes. *J. Am. Chem. Soc.* **115,** 6382 (1993).
2. B. O'Regan and M. Grätzel: A low-cost, high-efficiency solar-cell based on dye-sensitized colloidal TiO_2 films. *Nature* **353,** 737 (1991).
3. C.J. Bardé, F. Arendse, P. Comte, M. Jirousek, F. Lenzmann, V. Shklover, and M. Grätzel: Nanocrystalline titanium oxide electrodes for photovoltaic applications. *J. Am. Ceram. Soc.* **80,** 3157 (1997).
4. Y.F. Gao and M. Nagai: Morphology evolution of ZnO thin films from aqueous solutions and their application to solar cells. *Langmuir* **22,** 3936 (2006).
5. J.J. Wu, G.R. Chen, H.H. Yang, C.H. Ku, and J.Y. Lai: Effects of dye adsorption on the electron transport properties in ZnO-nanowire dye-sensitized solar cells. *Appl. Phys. Lett.* **90,** 213109 (2007).
6. J. Tornow and K. Schwarzburg: Transient electrical response of dye-sensitized ZnO nanorod solar cells. *J. Phys. Chem. C* **111,** 8692 (2007).
7. J. van de Lagemaat, K.D. Benkstein, and A.J. Frank: Relation between particle-coordination number and porosity in nanoparticle films: Implications to dye-sensitized solar cells. *J. Phys. Chem. B* **105,** 12433 (2001).
8. H. Lindstrom, A. Holmberg, E. Magnusson, S.E. Lindquist, L. Malmqvist, and A. Hagfeldt: A new method for manufacturing nanostructured electrodes on plastic substrates. *Nano Lett.* **1,** 97 (2001).
9. A. Ofir, T. Dittrich, S. Tirosh, L. Grinis, and A. Zaban: Influence of sintering temperature, pressing, and conformal coatings on electron diffusion in electrophoretically deposited porous TiO_2. *J. Appl. Phys.* **100,** 74317 (2006).
10. T. Dittrich, A. Ofir, S. Tirosh, L. Grinis, and A. Zaban: Influence of the porosity on diffusion and lifetime in porous TiO_2 layers. *Appl. Phys. Lett.* **88,** 182110 (2006).
11. *CRC Handbook of Chemistry and Physics* (CRC Press, Boca Raton, FL, 1991).
12. S. Kirkpatrick: Percolation and conduction. *Rev. Mod. Phys.* **45,** 574 (1973).
13. Y. Izyumov: Spin-wave theory of ferromagnetic crystals containing impurities. *Proc. Phys. Soc. London* **87,** 505 (1966).
14. J. Bernasconi and H.J. Wiesmann: Effective-medium theories for site-disordered resistance networks. *Phys. Rev. B* **13,** 1131 (1976).
15. K.D. Benkstein, N. Kopidakis, J. van de Lagemaat, and A.J. Frank: Influence of the percolation network geometry on electron transport in dye-sensitized titanium dioxide solar cells. *J. Phys. Chem. B* **107,** 7759 (2003).
16. S. Yamamoto, T. Sumita, Sugiharuto, A. Miyashita, and H. Naramoto: Preparation of epitaxial TiO_2 films by pulsed laser deposition technique. *Thin Solid Films* **401,** 88 (2001).